Electron Holography

Conner Stevons

Influenced by the work of William Bragg in X-ray crystallography, the physicist Dennis Gabor invented a new method of lensless imaging, now known as holography.[1] While holography is typically presented in the context of optical waves, Gabor was initially motivated to improve the resolving power of electron microscopes. His 1948 paper addresses the limitations that spherical aberrations from electron lenses pose on electron microscopy and proposes an experiment which discards the use of lenses. He theorizes using an electron beam that is brought to focus, with an object located after the focal point, partially obstructing the beam. This allows the unobstructed part of the reference beam to interfere with the obstructed part, and this interference recorded on a photographic plate.[2] Gabor recognized that recording the interference pattern between a coherent reference wave and a wave scattered by an object gives information on both the amplitude and phase of this scattered wave. Though the impact of his work was not fully appreciated at the time, the advent of lasers in the 1960s, which provided convenient coherent light sources, dramatically boosted its popularity in research teams around the world. Although the University of Michigan has an impressive history within the field optical holography, including Emmett Leith and Juris Upatnieks's work in synthetic aperture radar technology[3] and off-axis holography[4], it lies out of the scope of this report.

Due to the challenges of achieving a coherent source of electrons, electron holography matured much slower than optical holography.[5] Nevertheless, after the invention of field-emission guns which are able to produce beams with sufficient lateral coherence, holography has become an important technique used in electron microscopy. Its unique ability to record the spatial distributions of both intensity and phase of a sample[6] expands upon the information provided by typical S/TEM or SEM microscopy techniques, which only record intensity distributions. Such a technique thus allows one to, for example, quantitatively analyze magnetic and electrostatic potentials,[7] as well as mapping electrical, magnetic, and electromagnetic fields[8] with resolutions on the nanometer scale.

Before investigating recent progress in electron holography, it is worthwhile to mention a common denominator regarding the experimental setups seen in the literature using this technique. By far, the *electron biprism* is the most popular component employed in variants of off-axis holography.* This biprism is formed by a long, thin, conducting wire charged with a fixed voltage that is placed between two grounded plates, as shown in Figure 1(a).[9] The field distribution produced can be approximated to be the field created by a cylindrical capacitor.[10] With a positive voltage applied to the wire, it has been analytically and experimentally shown that the electron beams on either side of the wire are deflected toward the wire, independent of the impact parameter of each emitted electron (within a few microns).[11]† Consequently, the two deflected coherent beams will overlap in a region at the

---

*The differences between inline and off-axis holography can be found in many texts,[1] but one reason why off-axis holography is of focus in this report is its ability to separate the real and virtual images created from holography. In other words, when one image is brought into focus, the other is always out of focus, acting as an obscuration due to the inseparability of the images.

†For the seminal paper on the invention of the electron biprism, see Ref. (9). For an extensive theoretical analysis of the electron biprism, including a geometrical and wave interpretation of its effects, see Ref. (11).

observation plane which results in an interference pattern (see Figure 1(b)). If a specimen is placed within one of these beam paths above the electron biprism, this electron path will inherit an extra phase term with respect to the other path, and an interference pattern will be detected at the observation plane. The phase shift and intensity information is recorded in the positions of the interference fringes made in the resulting hologram. It should be noted that many of the setups seen in recent literature use either two (double-biprism holography)[12] or three (split-illumination holography)[13] biprisms, granting increased control over the propagation angles of the two electron waves, the interference width, and can lift some of the coherence length restrictions set by the thickness of the biprisms' charged wire.
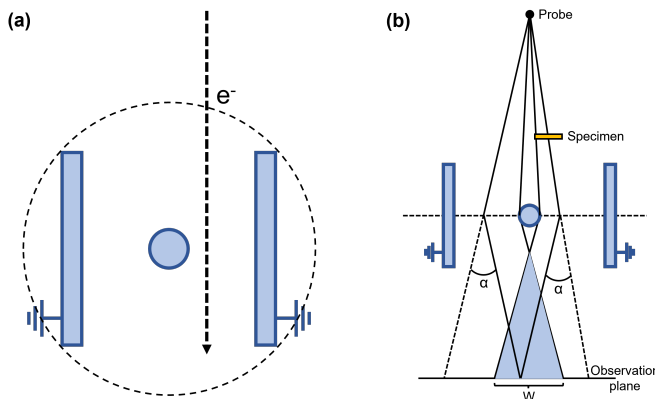

Figure 1: (a) Electron biprism consisting of a thin wire (oriented out of the paper) charged with a voltage, placed between two grounded plates running parallel to the electron beam. (b) Typical holographic experimental setup using an electron biprism. The angle α represents the deflection angle induced by the biprism on the electron beam and W represents the interference width. The shaded triangle represents the area where electron-wave interference occurs due to the splitting of the beam.

As previously mentioned here and discussed in class, electrons can be described quantum mechanically and, depending on the situation at hand, can be considered as behaving like a wave or a particle. Hence, the laws of optics can be applied to electron waves; however, electron holography can perform a broader set of measurements than what optical holography is capable of, especially in the context of materials. For instance, biochemical objects like viruses are classified as phase objects, meaning they tend to be transparent in conventional S/TEM imaging; staining or defocusing techniques are usually performed to achieve higher amplitude contrast.[14] Even so, as shown in Figure 2(a), staining and defocusing can blur image details, leading to selective adsorption around the object and ultimately to possible misclassifications within the image. Electron holography bypasses this. As seen in Figure 2(b), the phase image of the virus reconstructed from a TEM-based hologram is clearly visible without using stains. Furthermore, in another paper, the layer interfaces of different compositions of $Si_{1-x}Ge_x$ are easily distinguished from the phase image of a holographic setup, as opposed to a standard TEM image of the same stacked layers.[15]

Another extremely interesting application of electron holography is the three-dimensional mapping of electrostatic potential distributions using HR-TEM. In the context of semiconductors, when combining both electron holography and electron tomography, the three-dimensional electrostatic potential of homo- and heterojunctions can be quantitatively determined, which is shown to be directly related to their dopant distributions.[16] The authors of Ref. (16) prepared a Si p-n junction specimen using a FIB to concurrently rotate the
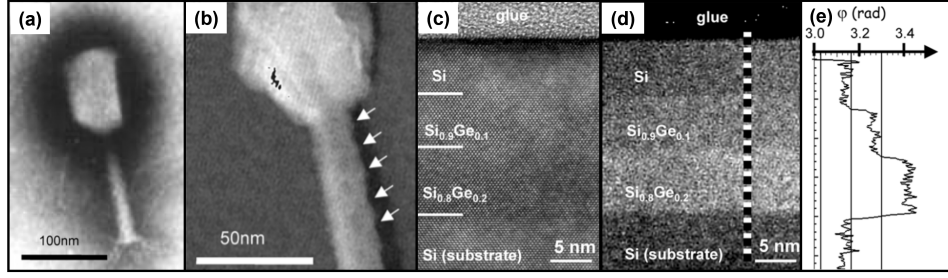
Figure 2: (a) TEM image of a stained T5-bacteriophage depicting the contrast obtained the edges of the specimen.[14] (b) Reconstructed phase image from a hologram of the an unstained virus.[15] The arrows point to the tail's helical structure, showcasing the high details that can be observed (c) The layers of $Si_{1-x}Ge_x$ are not distinguishable using conventional microscopy. (d) Reconstructed phase image of the same stacked layers of $Si_{1-x}Ge_x$, where the layers are clearly identified from their differing mean inner potentials. (e) A cross section of the mean inner potential, shown by the dashed line in (d).

specimen to high tilt angles in the TEM while maintaining an electrical bias across the specimen. Off-axis holograms were made over a tilt range of -70 to $+70°$ at $2°$ intervals, similar to what was done in our tomography lab assignments.[‡] Figure 3 in the appendix contains a schematic of the Si p-n junction, a reconstructed phase image (at a tilt angle of $+20°$) depicting the phase variation across the junction with an applied reverse bias of 3V, and the tomographic reconstruction of the electrostatic potential of the junction. An iterative back-propagation method (similar to a reconstruction method available in Tomviz applied in lab) was used to reconstruct the 3-D electric potential from the tilt series. The quantitative analysis of measuring the depletion width from the p-n junction electrostatic potential variation, as well as electric field and charge distributions can be obtained from holographic tomography technique, but unfortunately cannot fit into this report; please refer to Ref. (16) for these interesting details.

One last frontier in the field of electron holography that deserves attention is time-resolved off-axis holography using an ultrafast TEM (UEM). This technique allows one to record the temporal evolution of both the amplitude and phase of a signal, such as in characterizing dynamic ultrafast phenomena in nonlinear media with the aid of a femtosecond laser pulse.[17] To achieve high temporal resolution, one needs the capability of detecting light from these short pulses, especially so when attempting to capture ultrafast phenomena like the evolving electromagnetic fields in plasmonic structures.[8] This can be done in optical holography; however, using femtosecond lasers to create ultrafast electron pulses[18] gives us not only comparable temporal resolution with respect to optical techniques, but also a higher spatial resolution. Furthermore, implementing electron holography with this technique allows us to observe the phase dynamics of, say, electronic excitations in condensed matter, nonradiative energy transfer in molecules, and optical fields in metamaterials and photonic cyrstals.[8]

To conclude, the field of electron holography is a relatively new field that has much more room to grow. Higher temporal and spatial resolutions is an active avenue of research, which has tended to go hand-in-hand with the improvements being made with general electron microscopy imaging. The ability to reconstruct phase images of a specimen adds to the experimental repository of techniques that can be used to study materials, which useful in a vast number of fields including materials science.

[‡]A Philips CM300 FEG at an accelerating voltage of 200kV was used in Ref. (16).

References

[1] J. Goodman, *Introduction to Fourier Optics*. Roberts & Co. Publishers, 3rd ed., 2005.

[2] D. Gabor, "A new microscopic principle," *Nature*, vol. 161, pp. 777–778, 1948.

[3] E. Leith and J. Upatnieks, "Wavefront reconstruction and communication theory," *J. Opt. Soc. Am.*, vol. 53, p. 1123, 1962.

[4] E. Leith and J. Upatnieks, "Holograms: Their properties and uses," *SPIE J.*, vol. 4:3-6, 1962.

[5] H. Lichte and M. Lehmann, "Electron holography - basics and applications," *Rep. Prog. Phys.*, vol. 71, 2008.

[6] P. Midgley and R. Dunin-Borkowski, "Electron tomography and holography in materials science," *Nature Matter*, vol. 8, pp. 271–280.

[7] C. Ropers, "Holograms from electrons scattered by light," *Nature*, vol. 571, pp. 331–332.

[8] I. Madan, G. M. Vanacore, E. Pomarico, G. Berruto, R. J. Lamb, D. McGrouther, T. T. A. Lummen, T. Latychevskaia, F. J. G. de Abajo, and F. Carbone, "Holographic imaging of electromagnetic fields via electron-light quantum interference," *Sci. Adv.*, vol. 5, 2019.

[9] G. Möllenstedt and H. Düker, "Observations and measurements of biprism interference with electron waves," *Z. Phys.*, vol. 145, pp. 377–397.

[10] J. Komrska, "Scalar diffraction theory in electron optics," *Adv. Electron. Electron Phys.*, vol. 30, pp. 139–234.

[11] G. F. Missiroli, "Electron interferometry and interference electron microscopy," *J. Phys. E: Sci. Instrum.*, vol. 14, pp. 653–656.

[12] K. Harada, A. Tonomura, Y. Togawa, T. Akashi, and T. Matsuda, "Double-biprism electron interferometry," *Appl. Phys. Lett.*, vol. 84, p. 3229–3231.

[13] T. Tanigaki, Y. Inada, S. Aizawa, T. Suzuki, H. S. Park, T. Matsuda, A. Taniyama, D. Shindo, and A. Tonomura, "Split illumination electron holography," *Appl. Phys. Lett.*, vol. 101: 043101, 2012.

[14] A. Harscher, *Electron Holography of Biological Objects: Basics and Examples of Applications*. PhD thesis, University Tübingen, 1999.

[15] P. Formánek, *TEM-holography on Device Structures in Microelectronics*. PhD thesis, TU Cottbus, 2005.

[16] A. C. Twitchett-Harrison, T. J. V. Yates, S. B. Newcomb, R. E. Dunin-Borkowski, and P. A. Midgley, "High-resolution three-dimensional mapping of semiconductor dopant potentials," *Nano Lett.*, vol. 7, pp. 2020–2023.

[17] T. Balciunas, A. Melninkaitis, G. Tamosauskas, and V. Sirutkaitis, "Time-resolved off-axis digital holography for characterization of ultrafast phenomena in water," *Opt. Lett.*, vol. 33, pp. 58–60.

[18] A. Feist, N. Bach, N. R. da Silva, T. Danz, M. Möller, K. E. Priebe, T. Domröse, J. G. Gatzmann, S. Rost, J. Schauss, S. Strauch, R. Bormann, M. Sivisa, S. Schäfer, and C. Ropers, "Ultrafast transmission electron microscopy using a laser-driven field emitter: Femtosecond resolution with a high coherence electron beam," *Ultramicroscopy*, vol. 176, pp. 63–73.
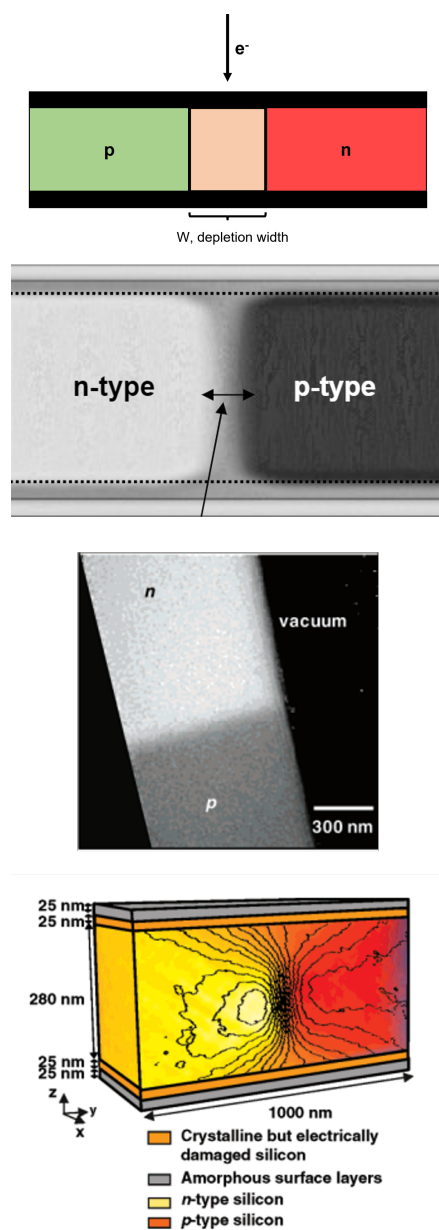
Appendices

Figure 3: (a) Schematic of a p-n junction similar to what is considered in Ref. (16). (b) The expected, computed potential variation of the FIB-prepared Si p-n junction specimen. (c) The reconstructed phase image (at a tilt angle of +20deg) of the p-n junction under an applied reverse bias of 3V. (d) The tomographic reconstruction of the FIB-prepared specimen. The superimposed equipotential contours shown are spaced every 0.2V, highlighting the potential distribution in this specimen cross section.

5